Molecular dipoles and tilted smectic formation: A Monte Carlo study

Roberto Berardi, Silvia Orlandi, and Claudio Zannoni
Dipartimento di Chimica Fisica ed Inorganica, Università di Bologna and INSTM, Viale Risorgimento 4, 40136 Bologna, Italy
(Received 7 November 2002; published 17 April 2003)

We investigate the possibility of forming a tilted smectic liquid crystal phase by suitably positioning two permanent dipoles in a rodlike molecule. We show, using Monte Carlo simulations, that a tilted smectic is formed from ellipsoidal Gay–Berne particles with two off-center outboard dipoles when these are directed along or at 60° from the rod axis where they are located, but not when they are perpendicular to it. The properties of the phases obtained are studied in some detail.

DOI: 10.1103/PhysRevE.67.041708 PACS number(s): 61.30.Cz, 61.30.Gd, 64.70.Md

I. INTRODUCTION

The smectic-*C* (S_C) phase is a layered liquid crystalline phase in which constituent molecules are on average tilted with respect to the layer plane, while their centers of mass have no positional order [1–3] and in this sense it is a tilted analog of the smectic-*A* phase. Tilted versions exist also for the smectic-*B* phase, where a local hexagonal order in the position of the molecules exists. Although there is no *a priori* reason to exclude certain tilt directions, the tilt in a layer is typically found to be along one the lines connecting two nearest neighbors (smectic-*I* phase) or perpendicular to it (smectic-*F* phase). The same occurs for the crystal-like analogs of the smectic-*B* phase, where the hexagonal order has a long-range correlation (smectic-*J*, smectic-*G*). Although tilted phases and smectic-*C* phase in particular are of considerable importance for electro-optical devices, the molecular origin of their somewhat counterintuitive organization is still largely unknown.

The first successful theory of smectic-*C* liquid crystals, the mean field theory of McMillan [4], related the formation of the tilted phase to the presence of at least two outward pointing dipoles in the mesogenic molecule. Permanent or induced dipoles have been the key molecular ingredient of various other approximate theoretical treatments [5–9], although there is no consensus on a set of features sufficient to guarantee tilt. Thus, e.g., van der Meer and Vertogen [6] considered the induction forces between transverse dipoles and neighboring polarizable centers, while in a recent treatment by Govind and Madhusudana the off-axis position of a single transversal permanent dipole has been considered the key feature for tilt [9]. Although it is known, since the synthetic work of Goodby *et al.* [10], that the presence of two or even one dipole is not a mandatory requirement, and that smectic-*C* phase can be formed even without these features, the vast majority of *C* smectogens is polar and it is interesting to study to what extent a nonapproximate approach, like the Monte Carlo (MC) computer simulations employed here, can yield or not tilted phases for dipolar systems. In particular, if smectic-*C* phase or other tilted phases can be obtained, it is interesting to establish a relation between molecular features, such as dipole positions and orientations, that can be controlled at the synthesis level, and phase behavior. The structure of the dipole based tilted phase is interesting also in relation to the issue of an effective locking or not of the molecular dipoles in the biaxial smectic-*C* structure. A strong freezing of rotations around the long axis of the molecule more or less implicit in the earlier theoretical treatments [5] was ruled out by NMR measurements in the smectic-*C* phase [11] and, by neutron scattering, in the smectic-*H* phase, a nearly crystalline tilted phase with herringbone structure [2,12].

Although some atomistic simulations of tilted smectics have appeared [13,14], the equilibration times are so long that only small samples preliminarly prepared in a layered situation could be studied and certainly molecular rather than atomistic level simulations are more appropriate for the type of study we are interested in here. The prototype model for the simulation at molecular size resolution of liquid crystals is the so called Gay-Berne (GB) potential [15,16], an anisotropic, ellipsoidal shape, version of the attractive-repulsive Lennard-Jones interaction for spherical particles. The GB model has been shown to be capable of reproducing, by suitably tuning of shape and attractive anisotropies, nematic, smectic-*A* and smectic-*B* phases (see Ref. [17] for a recent review). Extensive simulations of GB particles with an embedded dipole have been performed by various groups [18–26] and have yielded most of the complex polymorphism for polar smectics, including striped [18], interdigitated and bilayer phases [19]. However, it is worth noticing that simulations of GB systems without or with only one dipole at various positions and orientations, have never convincingly shown tilted phases. Indeed earlier claims of tilted smectics, being observed in systems of apolar [27], transversal [21] and axial [22] monodipole GB, are probably due to small and fixed size samples and to the too limited duration of the simulations [22,28].

Other theoretical models considered to try and obtain smectic-*C* phase have been based on molecular shape and in particular on a zigzag shape [29–34]. While a zigzag shape is probably important for real molecules with flexible end chains [14,31], the simple model particles, built by assembling in a zigzag way GB particles, have not shown tilted phase formation [32]. A zigzag model made of seven soft repulsive spheres with the two terminal ones at an angle of 45° from the five in line core ones showed a smectic-*C* behavior with random tilt orientation, although an elaborate equilibration procedure had to be used [34]. A zigzag in-

ϕ	d^*
90°	1.0
75°	1.0
60°	1.0
60°	1.2
0°	1.0

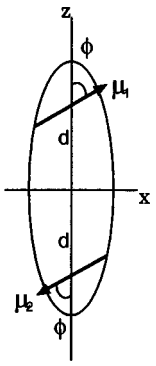

FIG. 1. A sketch of the molecular model employed in this work, showing position and orientation of the two permanent dipoles within a Gay-Berne ellipsoidal particle. The values of ϕ and d^* explored in this work are shown in the table.

spired model (called ''IRTO'') consisting of a single site GB potential in which the attractive minima are twisted with respect to the axis normal of an angle δ, shows tilted smectic-J (S_J) phase, for $\delta \geqslant 30°$, for aspect ratio 3:1 and smectic-G (S_G) phase for 4:1 [35].

The interaction between molecular quadrupoles has also been considered as a possible source of tilt. The addition of a transverse quadrupole [36] to GB particles only stabilizes smectic-A, -B phases. However, molecular dynamics simulations by Neal and Parker [37] have shown formation of a smectic-C phase for central axial quadrupoles of weak or moderate strength, while high magnitude point quadrupoles destabilize the smectic phase formation. The tilting effect of

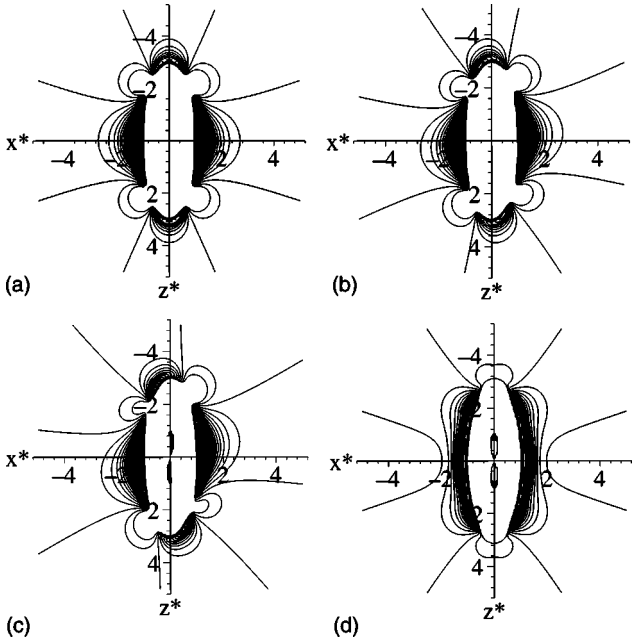

FIG. 2. Potential energy contours U_{ij}^* obtained with a molecule at the origin with long axis oriented along laboratory Z and a second one parallel to the first exploring the X-Z plane for $d^*=1$, and (a) $\phi=90°$; (b) $\phi=75°$; (c) $\phi=60°$; (d) $\phi=0°$. Molecular dipoles are laying on the X-Z plane and dimensionless units are used.

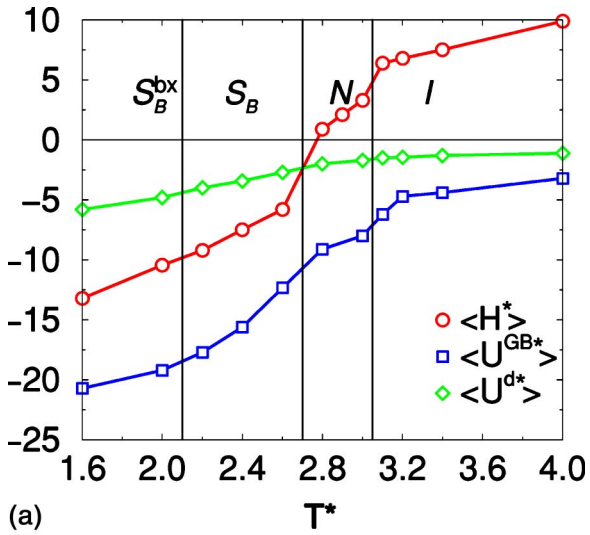

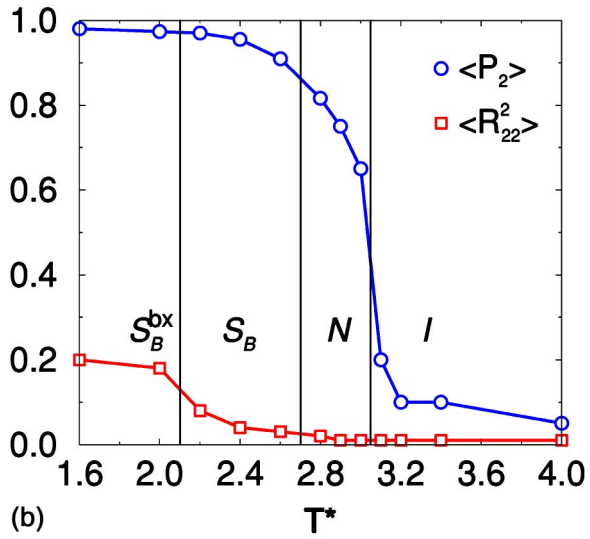

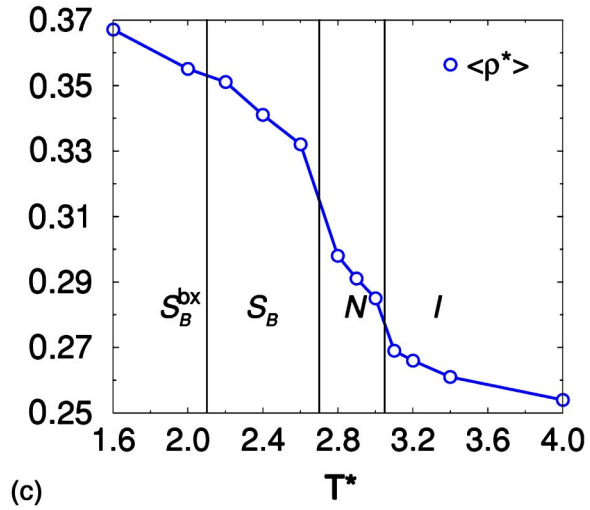

FIG. 3. Average enthalpy $\langle H^* \rangle = \langle U^* \rangle + P^* \langle V^* \rangle$, Gay-Berne $\langle U^{GB*} \rangle$ and dipolar $\langle U^{d*} \rangle$ energy terms per particle (a), orientational $\langle P_2 \rangle \equiv \langle R_{00}^2 \rangle$ and biaxial $\langle R_{22}^2 \rangle$ order parameters (b), and number density $\langle \rho^* \rangle = N\sigma_s^3 \langle 1/V \rangle$ (c), as a function of temperature T^*, for a system of $N=1000$ dipolar GB rods with $\phi=90°$ and $d^*=1$.

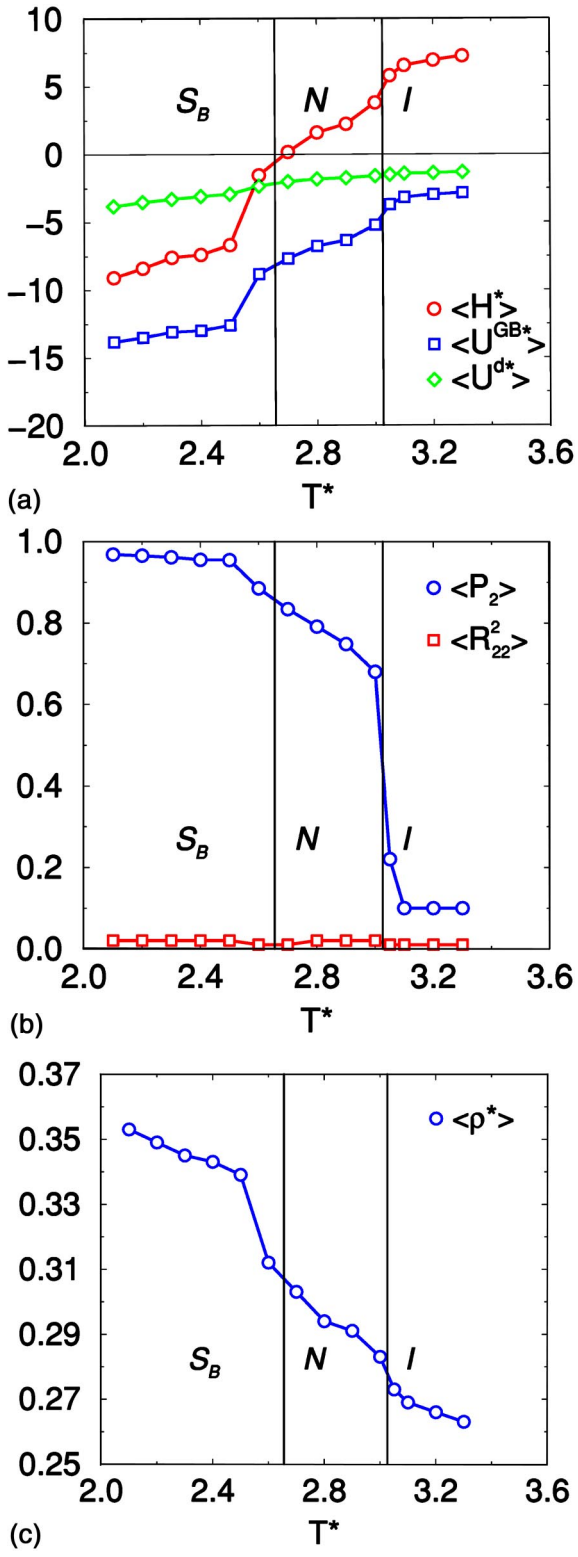

FIG. 4. System of $N=1000$ dipolar GB rods with $\phi=75°$ and $d^*=1$; see Fig. 3 for additional details.

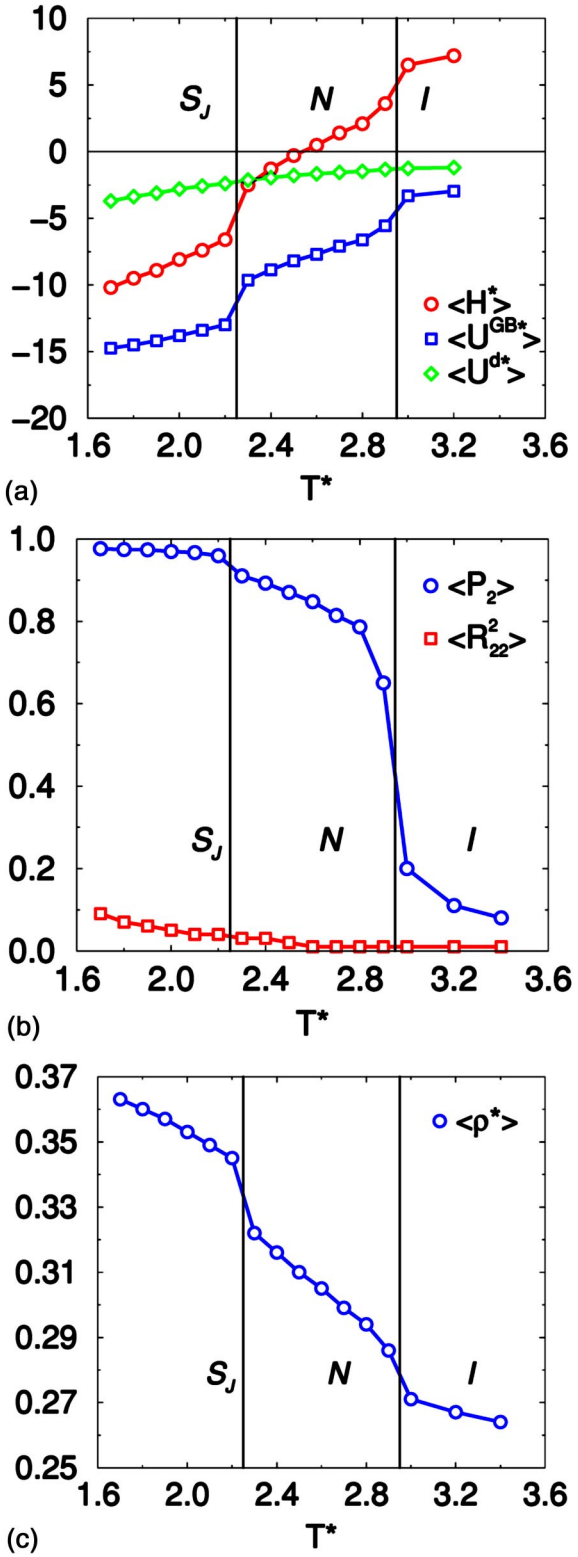

FIG. 5. System of $N=1000$ GB rods with $\phi=60°$ and $d^*=1$; see Fig. 3 for additional details.

quadrupoles can well be due to energetic reasons, as the potential minimum for two axial quadrupoles, sliding parallel to each other, occurs when the intermolecular vector is tilted from the molecular normal [38,39]. Adding a quadrupole to the already mentioned IRTO model also yielded tilted phases [35].

Given this large number of works, it is somewhat surprising that the original model of a particle with multiple dipoles

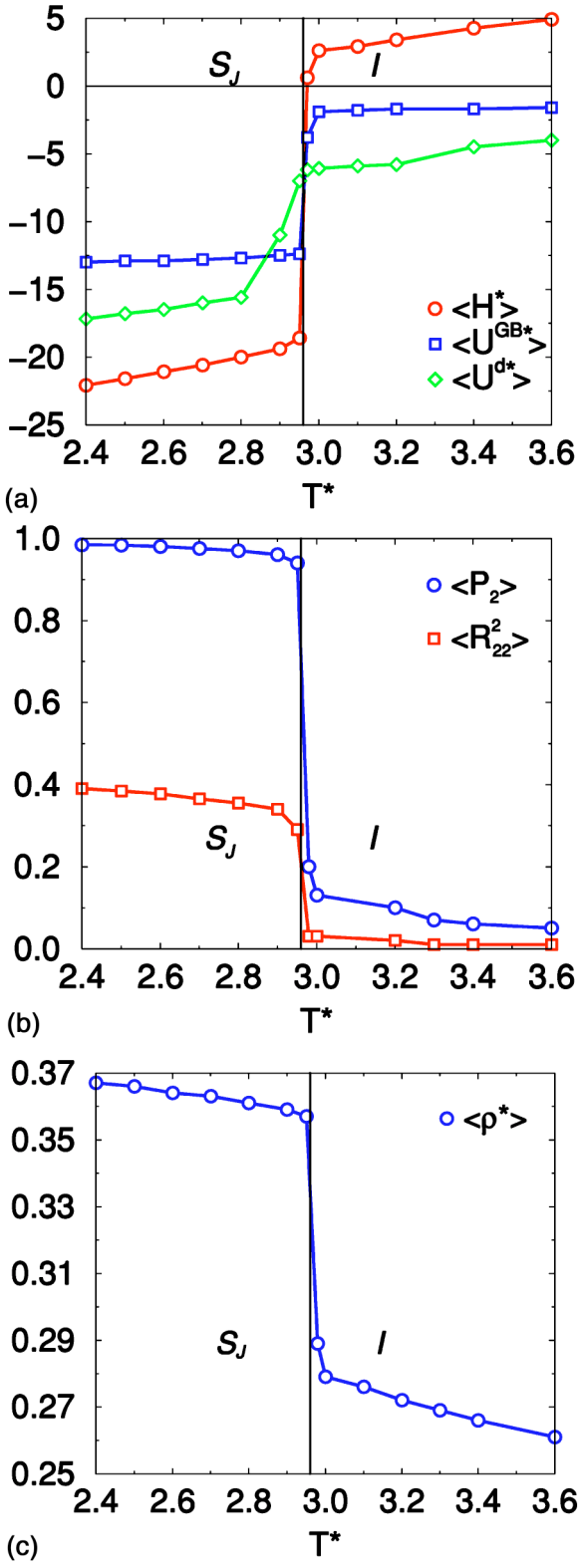

FIG. 6. System of $N=1000$ GB rods with $\phi=60°$ and $d^*=1.2$; see Fig. 3 for additional details.

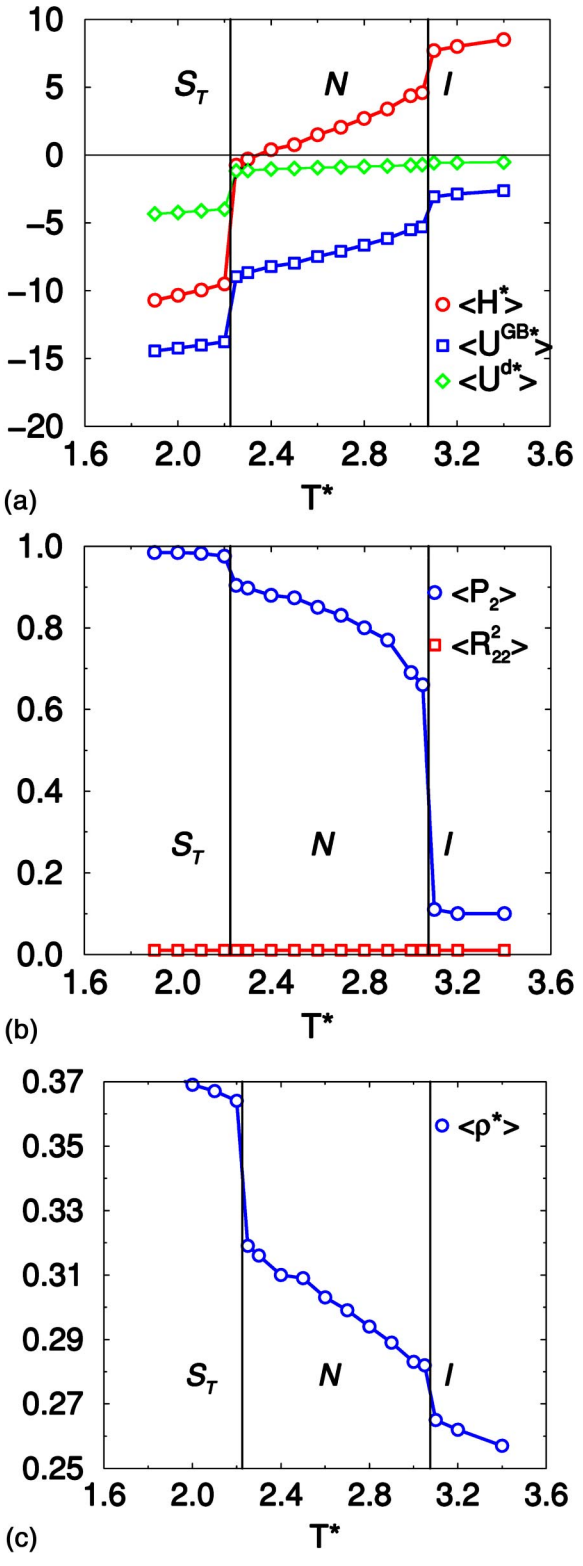

FIG. 7. System of $N=1000$ GB rods with $\phi=0°$ and $d^*=1$; see Fig. 3 for additional details.

has, to the best of our knowledge, not been studied by computer simulations. Here, we have thus considered a system of Gay-Berne molecules [15] with two embedded dipoles at different orientations with respect to the long molecular axis and located at selected positions between the center and the end of the molecule. For each case we have investigated several temperatures corresponding to nematic and smectic liquid crystal phases, using constant pressure MC simula-

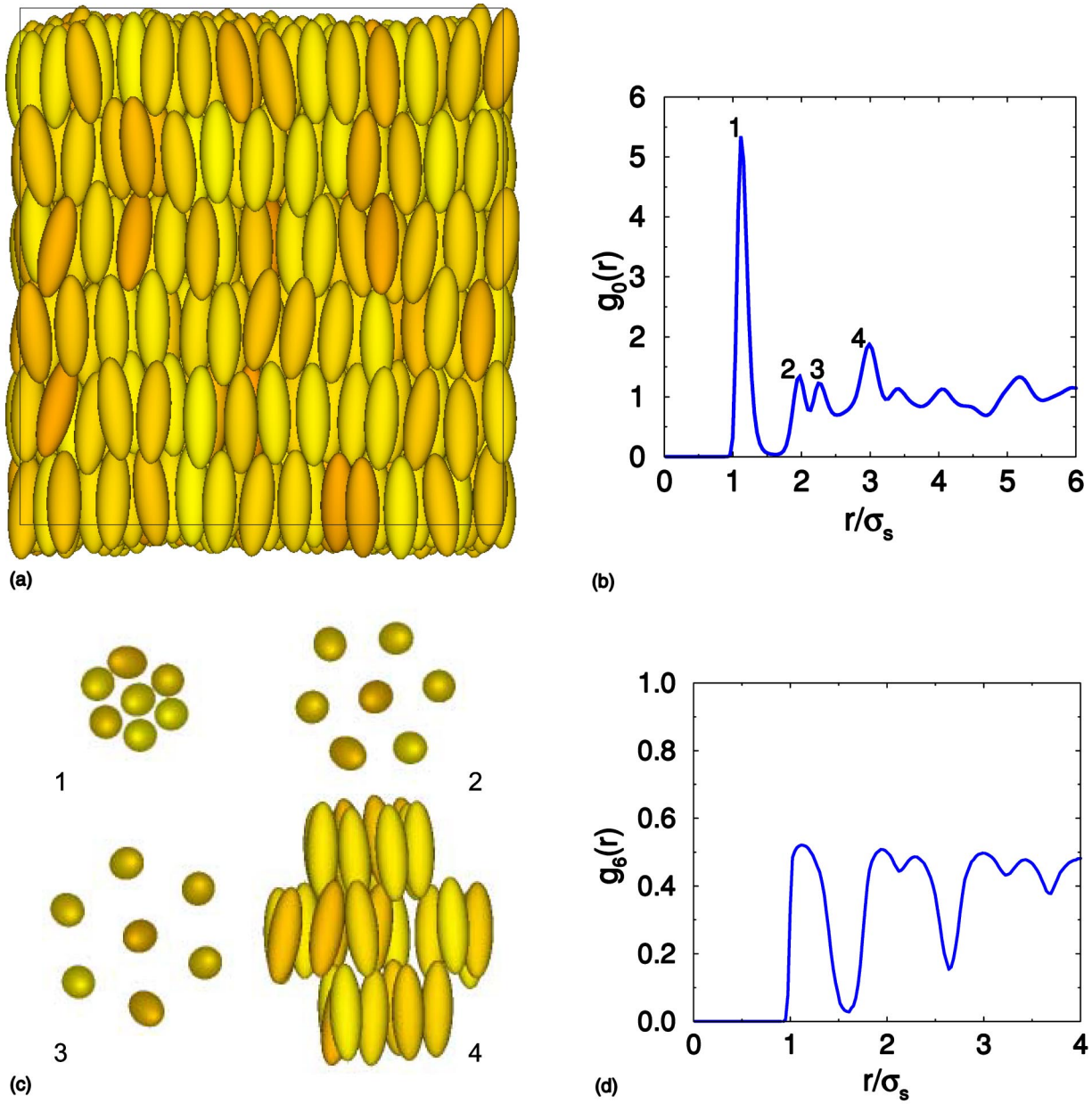

FIG. 8. Snapshot of the MC sample taken from the X director frame axis (a), radial correlation function $g_0(r)$ (b), and bond-correlation function $g_6(r)$ (d), for a system with dipolar orientation $\phi=90°$, and position $d^*=1$ at $T^*=2.0$. The labels on the maxima of $g_0(r)$ correspond to the typical organizations shown in the pictures in plate (c).

tions, trying to establish a relation between dipoles configuration and tilting effect. We have also tried to characterize and assign the tilted smectic phases obtained, that are found to be particularly sensitive to the dipolar configuration.

II. MODEL

We consider a system of uniaxial ellipsoidal particles of length σ_e, width σ_s and $\sigma_e=3\,\sigma_s$, with two embedded electric point dipoles $\boldsymbol{\mu}_1$ and $\boldsymbol{\mu}_2$ located at dimensionless position $d^*\equiv d/\sigma_s$, $(0,0,d^*)$, and $(0,0,-d^*)$ with orientation ϕ, $180°+\phi$ with respect to the long molecular axis (Fig. 1). The pair potential is the sum of a Gay-Berne [15,40] and a dipole-dipole term: $U_{ij}^*\equiv U_{ij}/\epsilon_s=U_{ij}^{GB}{}^*+U_{ij}^d{}^*$. The Gay–Berne term has a repulsive and attractive contribution with a 12-6 inverse distance dependence form

$$U_{ij}^{GB}{}^*=4\epsilon(\mathbf{z}_i,\mathbf{z}_j,\hat{\mathbf{r}})\left[\left\{\frac{\sigma_s}{r-\sigma(\mathbf{z}_i,\mathbf{z}_j,\hat{\mathbf{r}})+\sigma_s}\right\}^{12}-\left\{\frac{\sigma_s}{r-\sigma(\mathbf{z}_i,\mathbf{z}_j,\hat{\mathbf{r}})+\sigma_s}\right\}^{6}\right], \tag{1}$$

where $\mathbf{z}_i$ and $\mathbf{z}_j$ are the molecular orientations, $\mathbf{r}=r\hat{\mathbf{r}}=\mathbf{r}_j-\mathbf{r}_i$ is the intermolecular vector, $\sigma(\mathbf{z}_i,\mathbf{z}_j,\hat{\mathbf{r}})$ is the contact

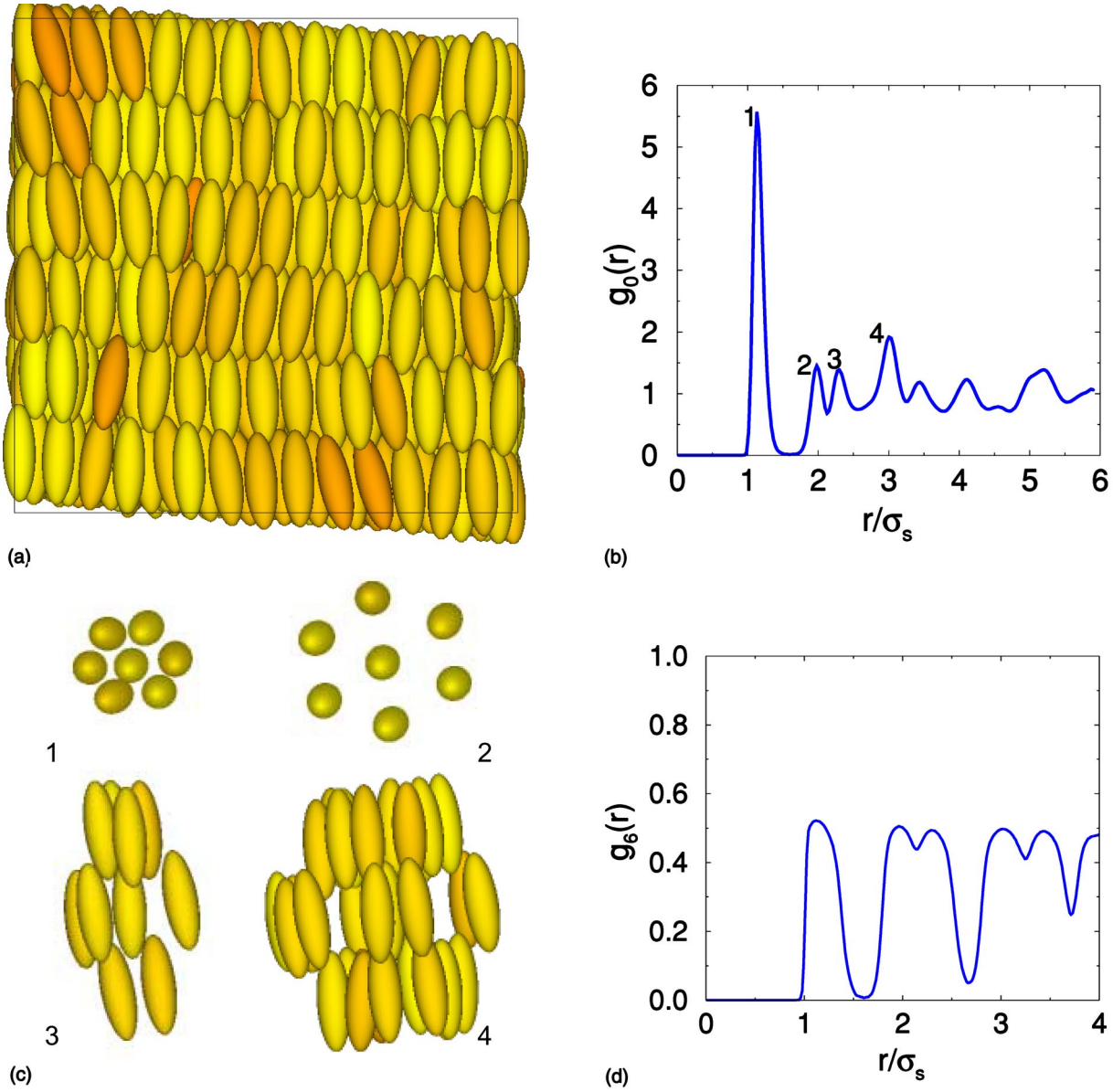

FIG. 9. Snapshot of a MC sample taken from the X director frame axis (a), radial correlation function $g_0(r)$ (b), and bond-correlation function $g_6(r)$ (d), for a system of GB particles with dipolar orientation $\phi=60°$ and position $d^*=1$ at $T^*=1.8$. The labels on the maxima of $g_0(r)$ correspond to the typical organizations shown in the pictures in plate (c).

distance, $\epsilon(\mathbf{z}_i,\mathbf{z}_j,\hat{\mathbf{r}})$ is the interaction energy defined as in Refs. [15,40], and containing two further tuning parameters μ and ν. Here we employ the GB parameters $\mu=1$, $\nu=3$ and potential well anisotropy $\epsilon_s/\epsilon_e=5$ that shows a wide nematic, a smectic-A (S_A) and smectic-B (S_B) phase [40].

The dipolar energy is a sum of contributions given by the classic electrostatic expression:

$$U_{ij}^{d*}=\sum_{\alpha\in i,\beta\in j}\frac{\sigma_s^3}{r_{\alpha\beta}^3}[\boldsymbol{\mu}_{i,\alpha}^*\cdot\boldsymbol{\mu}_{j,\beta}^*-3(\boldsymbol{\mu}_{i,\alpha}^*\cdot\hat{\mathbf{r}}_{\alpha\beta})(\boldsymbol{\mu}_{j,\beta}^*\cdot\hat{\mathbf{r}}_{\alpha\beta})], \tag{2}$$

where $\mathbf{r}_{\alpha\beta}$ is the vector joining two point dipole moments $\boldsymbol{\mu}_{i,\alpha}^*$ and $\boldsymbol{\mu}_{j,\beta}^*$ on molecules i and j. We have assumed a dimensionless moment $\mu^*\equiv(\mu^2/\epsilon_s\sigma_s^3)^{1/2}=1$, corresponding to $\approx 1.3D$ if we take $\sigma_s=5$ Å and an energy scale $\epsilon_s/k_B=100$ K. As we shall see, this provides a significant but not overwhelming perturbation over the GB potential.

The potential energy contours U_{ij}^*, obtained with a molecule at the origin oriented along Z and a second one parallel to the first exploring the X-Z plane, are plotted in Fig. 2. In this representation, the shape of the molecules corresponds essentially to the zero potential energy contours. We have considered four dipole orientations, keeping the same dipole positions ($d^*=1$): (a) with dipoles perpendicular to the long molecular axis, $\phi=90°$, then (b) with dipoles tilted to $\phi=75°$ and (c) $\phi=60°$, and eventually (d) with axial, antiparallel dipoles, $\phi=0°$. An additional set of simulations was

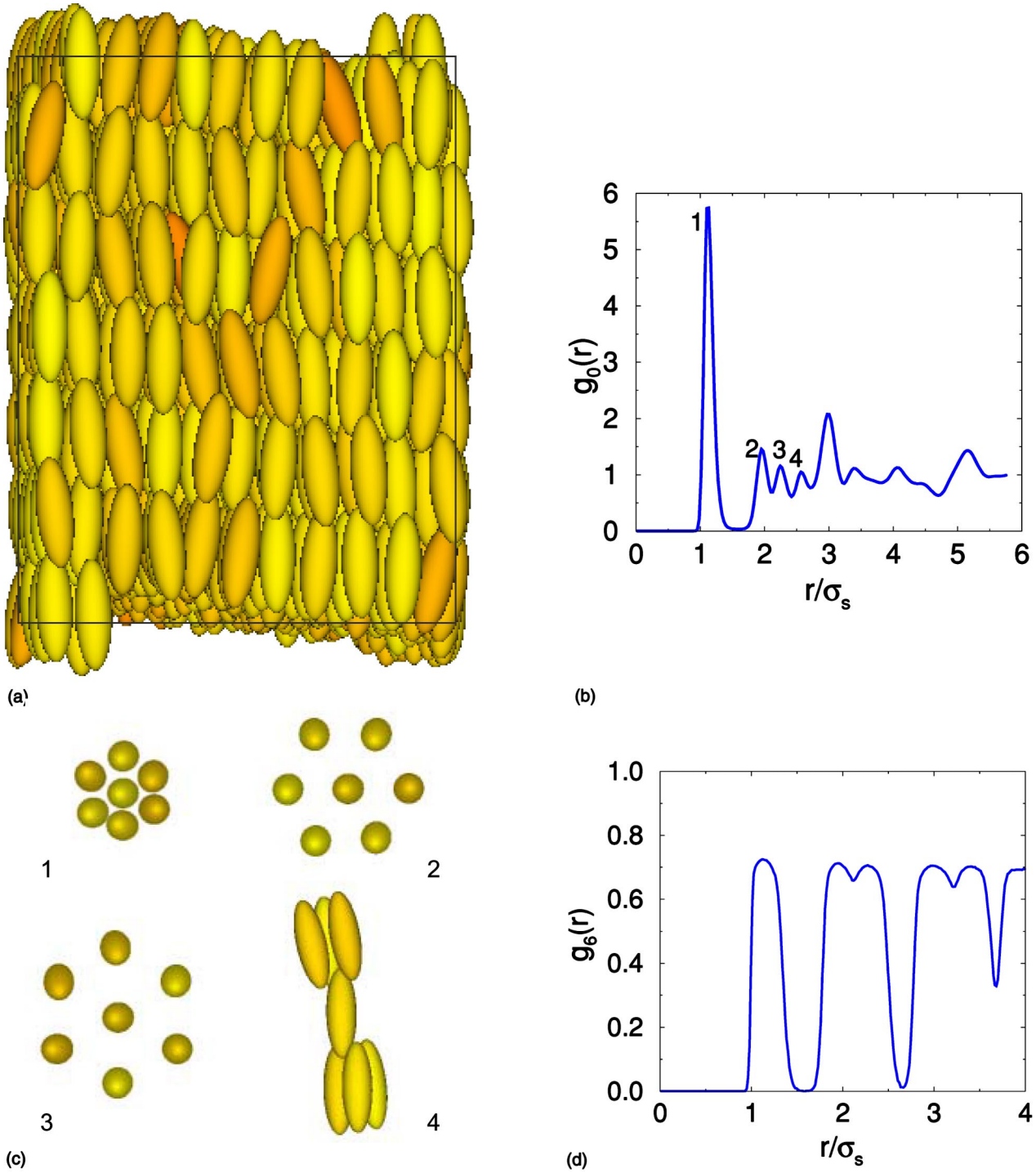

FIG. 10. Snapshot of a MC sample taken from the X director frame axis (a), radial correlation function $g_0(r)$ (b) and bond-correlation function $g_6(r)$ (d), for a system with dipolar orientation $\phi=60°$ and position $d^*=1.2$ at $T^*=2.7$. The labels on the maxima of $g_0(r)$ correspond to the typical organizations shown in the pictures in plate (c).

performed for dipoles at $\phi=60°$ moving the dipoles in a more terminal position at $d^*=1.2$.

III. MONTE CARLO SIMULATIONS AND OBSERVABLES

We have performed Monte Carlo simulations of a system of $N=1000$ particles in the isobaric-isothermal (NPT) ensemble (constant number of molecules N, dimensionless pressure $P^*\equiv P\sigma_s^3/\epsilon_s=6$ and dimensionless temperature $T^*\equiv k_BT/\epsilon_s$), using periodic boundary conditions. The MC runs were started from well equilibrated isotropic configurations of the dipole-less system and a cubic box with dimensionless volume $V^*=V/\sigma_s^3$. After switching on the dipoles, the simulations were run in a cooling sequence with equili-

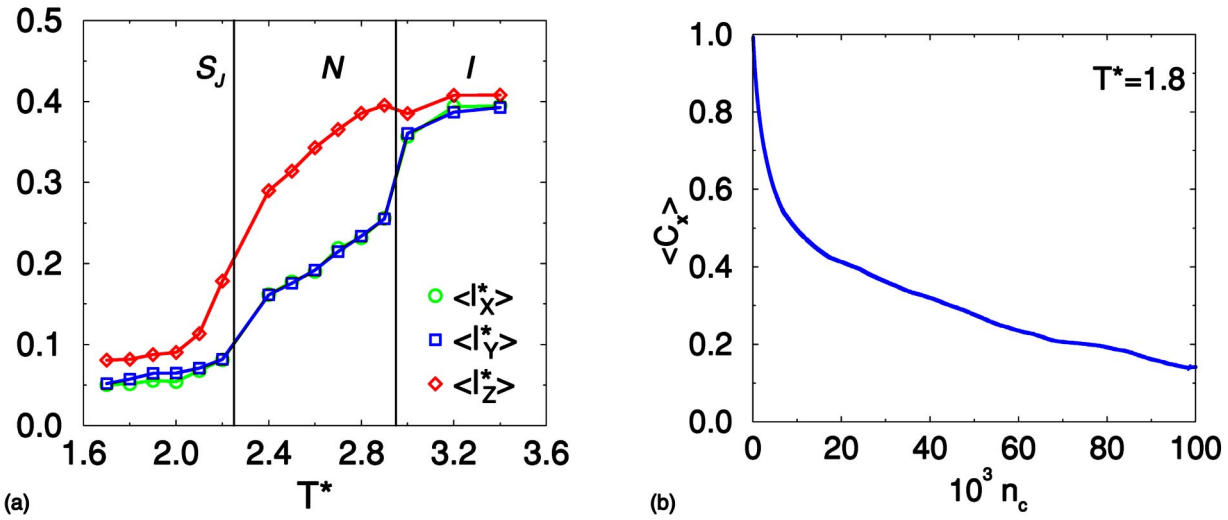

FIG. 11. Average mean square displacements $\langle l_X^* \rangle$, $\langle l_Y^* \rangle$, and $\langle l_Z^* \rangle$ (a), and autocorrelation function for reorientation around the molecular axis $\langle C_x \rangle$ at $T^*=1.8$ (b), for the case $\phi=60°$ and $d^*=1.0$.

bration runs of ≈ 300 kcycles, where a cycle corresponds to N attempted MC moves. The box shape was adjusted during volume update moves. As soon as the ordered phase was reached, the whole sample was rotated, together with its periodic images, in order to have the director axis parallel to the laboratory Z one; then the equilibration runs were continued. We have also allowed the dipoles to flip of 180° around the molecular z_i and x_i axes. In practice, flip moves are attempted with probability 0.2. Production runs, during which observables were accumulated for averaging and data analysis, were usually 200 kcycles long. Runs without flip moves have also been performed, both as a check and to examine dipole reorientation around the long molecular axis.

The electrostatic energy has been evaluated using the reaction field method [41] that has been extensively tested by other researchers [23,24] and by us [19,25,26] in previous simulations of dipolar systems and found to be satisfactory, with results similar to those of full Ewald summations, for samples as big as the present ones.

We have determined from the simulations the usual thermodynamic quantities, average enthalpy $\langle H^* \rangle$, energies $\langle U^{GB*} \rangle$ and $\langle U^{d*} \rangle$, and orientational order parameters appropriate for a potentially biaxial system [42,43], i.e., $\langle R^2_{0,0} \rangle = \langle P_2 \rangle = \langle (3\cos^2\beta - 1)/2 \rangle$, $\langle R^2_{2,0} \rangle = \langle \sqrt{3/8} \sin^2\beta \cos 2\alpha \rangle$, and $\langle R^2_{2,2} \rangle = \langle (1+\cos^2\beta)(\cos 2\alpha \cos 2\gamma)/4 - (\cos\beta \sin 2\alpha \sin 2\gamma)/2 \rangle$, where α, β, and γ are the Euler angles giving the orientation of the molecular axis system (x,y,z) in the laboratory frame (X,Y,Z).

Notice that the biaxial order parameter $\langle R^2_{2,2} \rangle$ is different from zero only for biaxial molecules and phases, while $\langle R^2_{2,0} \rangle$ is in principle different from zero also for a biaxial phase of uniaxial molecules. In all the systems studied, $\langle R^2_{2,0} \rangle$ was zero within our statistical error, thus we do not explicitly report it. This is probably due to the fact that even for phases with small tilt angle, the director is very close to the layer normal, so that $\beta \approx 0°$ giving a very small $\langle R^2_{2,0} \rangle$ order parameter even for high biaxiality.

We characterize the structures obtained first of all through the radial correlation function $g_0(r)$

$$g_0(r) = \frac{1}{4\,\pi r^2 \rho} \langle \delta(r - r_{ij}) \rangle_{ij}, \tag{3}$$

where the average $\langle \ldots \rangle_{ij}$ is computed over all molecular pairs.

In the smectic phases, we have calculated the average tilt angle $\langle \theta \rangle$, that is the angle between the phase director $\mathbf{Z}$ and the normal $\mathbf{n}$ to the layers. The procedure consists in locating the layer normal $\mathbf{n}$ by means of a geometrical method. In practice, a molecular layer is defined as the set of particles for which the first-neighbors distance is $r \leqslant 1.3\sigma_s$. For each layer plane k, that can be expressed by the equation $A_k x + B_k y + C_k z + D_k = 0$, the direction cosines A_k, B_k, and C_k are determined with a least-squares method. Hence, the normal $\mathbf{n}$ is obtained from the averages A, B, and C of these local cosines for a single MC configuration. The tilt angle is calculated as an average over all configurations: $\langle \theta \rangle \equiv \langle \cos^{-1}(\mathbf{Z} \cdot \mathbf{n}) \rangle$.

We also calculate, where necessary to characterize the smectic phases obtained, the global hexatic order parameter $\langle \psi_6 \rangle$, average of the parameter ψ_6 for one MC configuration [44]:

$$\psi_6 = \frac{1}{N_k} \sum_{m=1}^{N_k} \psi_{6m} \tag{4}$$

with N_k the number of molecules in the layer, which is in turn the sample average of the local hexatic order and

$$\psi_{6m} = \frac{1}{N_m} \sum_{n=1}^{N_m} e^{i6\theta_{mn}} \tag{5}$$

with the sum running over the N_m nearest neighbors of molecule m, and θ_{mn} the angle between position vector $\mathbf{r}_{mn}$ and

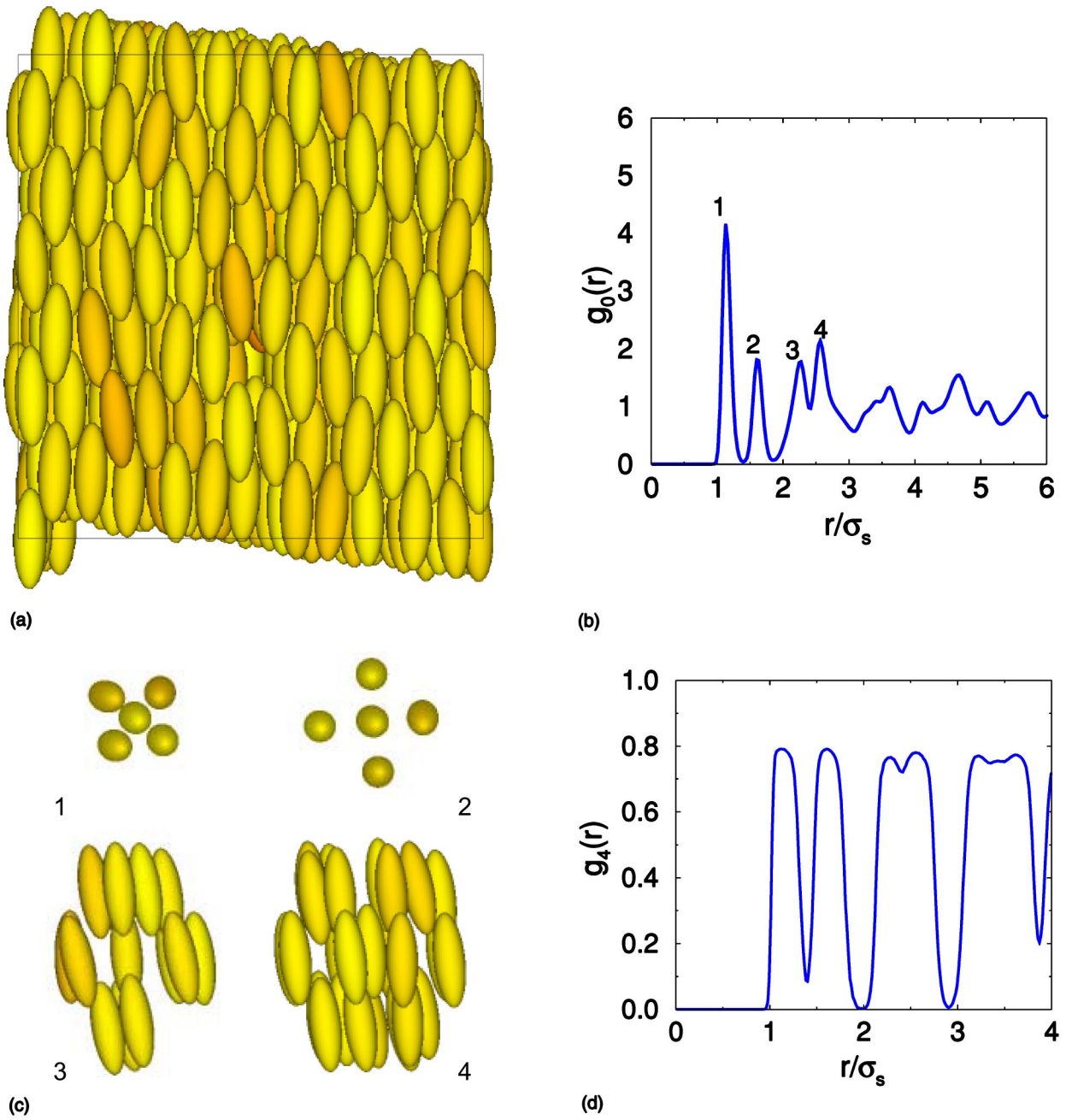

FIG. 12. Snapshot of a MC sample taken from the *X* director frame axis (a), radial correlation function $g_0(r)$ (b), and bond-correlation function $g_4(r)$ (d), for a system with dipolar orientation $\phi=0°$ and position $d^*=1$ at $T^*=2.0$. The labels on the maxima of $g_0(r)$ correspond to the typical organizations shown in the pictures in plate (c).

an arbitrary fixed axis passing through *m*. The correlation between the local hexatic order of two particles *i* and *j* separated by a vector $\mathbf{r}_{ij}$ at various positions in the same layer is measured by the bond-orientational correlation function

$$g_6(r)=\left\langle \sum_{i\neq j} \psi_{6i}\psi_{6j}^{*}\delta(r-r_{ij})\right\rangle \Big/ \left\langle \sum_{i\neq j} \delta(r-r_{ij})\right\rangle. \tag{6}$$

This will be particularly useful to differentiate between the case of smectic-*C* phase, where $g_6(r)$ is expected to be short range, and the more crystal-like smectic-*F*, *G*, *I*, *J* phase, where $g_6(r)$ should be long range.

IV. RESULTS

We plot in Figs. 3–7, the temperature dependence of average enthalpy and energies per particles, uniaxial and biaxial order parameters, and number density for the five systems studied, while numerical tables of the observables and phase assignments are reported in subsequent tables. From the plots we see at once that all systems studied have ordered phases.

TABLE I. Results from MC–*NPT* simulations at pressure $P^*=6$ for a system of $N=1000$ GB rodlike molecules with two dipoles with orientation $\phi=90°$, position $d^*=1$, and module $\mu^*=1$. We report the average Gay-Berne $\langle U_{ij}^{GB}{}^*\rangle$ and the dipolar $\langle U_{ij}^{d}{}^*\rangle$ energies per particle, the orientational $\langle R_{00}^2\rangle$ and the biaxial $\langle R_{22}^2\rangle$ order parameters, as well as the hexatic order parameter $\langle \psi_6\rangle$, at temperatures T^* corresponding to isotropic (I), nematic (N) and smectic-B (S_B) phases as indicated. All quantities are dimensionless. The average layer normal tilt angle $\langle \theta\rangle$ was zero at all temperatures studied.

T^*	$\langle U_{ij}^{GB}{}^*\rangle$	$\langle U_{ij}^{dd}{}^*\rangle$	$\langle R_{00}^2\rangle$	$\langle R_{22}^2\rangle$	$\langle \psi_6\rangle$	Phase
1.6	-20.7 ± 0.2	-5.8 ± 0.1	0.98 ± 0.01	0.20 ± 0.02	0.73 ± 0.02	S_B bx
2.0	-19.2 ± 0.2	-4.8 ± 0.1	0.97 ± 0.01	0.18 ± 0.02	0.68 ± 0.02	S_B bx
2.2	-17.7 ± 0.2	-4.0 ± 0.1	0.97 ± 0.01	0.08 ± 0.02	0.63 ± 0.02	S_B
2.4	-15.6 ± 0.2	-3.4 ± 0.1	0.96 ± 0.01	0.04 ± 0.02	0.61 ± 0.02	S_B
2.6	-12.3 ± 0.2	-2.7 ± 0.1	0.91 ± 0.01		0.55 ± 0.02	S_B
2.8	-9.1 ± 0.2	-2.0 ± 0.1	0.82 ± 0.01			N
3.0	-8.0 ± 0.2	-1.7 ± 0.1	0.75 ± 0.01			N
3.1	-6.2 ± 0.2	-1.5 ± 0.1	0.65 ± 0.01			N
3.2	-4.7 ± 0.2	-1.4 ± 0.1	0.2 ± 0.01			I
3.4	-4.4 ± 0.2	-1.3 ± 0.1	0.1 ± 0.01			I
4.0	-3.2 ± 0.2	-1.1 ± 0.1	0.1 ± 0.01			I

However, the number and type of these phases vary significantly. In particular, tilted phases are only obtained when the two dipoles make an angle $\phi\leqslant 60°$ with the long molecular axis. In Figs. 8(a), 9(a), 10(a), and 12(a), we show typical snapshots (suitably rotated with the director **Z** along the vertical direction) of the low temperature smectic phases obtained for $d^*=1$ and $\phi=90°$, $\phi=60°$, $\phi=0°$, and $d^*=1.2$, $\phi=60°$. From the plots of the polar and Gay-Berne contributions to the energy [Figs. 3(a)–7(a)], we see that in none of the cases studied the dipolar contribution is dominant and represents at most a 30% of the Gay-Berne energy. We now briefly comment on each of the various systems studied.

For $\phi=90°$, the phase sequence [Fig. 3(b)] is similar to the dipole-less GB one with isotropic, nematic, and smectic-B phase but with the addition of an orthogonal biaxial smectic phase (S_B^{bx}) at low temperature. This phase has hexatic order, with $\langle \psi_6\rangle\approx 0.7$ at the two biaxial temperatures studied (see Table I) as we can also see from the analysis of the peaks in the radial distribution, shown in Figs. 8(b) and 8(c), and from the bond-orientational correlation function in Fig. 8(d). Although we have previously seen biaxial smectics (and nematics) for GB particles with biaxiality in their attractive and repulsive interactions [43], we notice that here the biaxiality comes exclusively from the presence of the dipoles. Examining a typical snapshot [Fig. 8(a)] and the radial distribution $g_0(r)$ [Figs. 8(b)], we see that the smectic structure is not interdigitated and shows a pronounced peak at $r^*=3$ corresponding to two molecules, one on top of the other. For an angle $\phi=75°$, all the ordered phases observed are uniaxial [Fig. 4(b) and Table II]. A smectic-B phase with hexatic order $\langle \psi_6\rangle\geqslant 0.6$ is obtained for $T^*=2.2$. Figures 3(a) and 4(a) show that in the two cases where a tilted phase is not observed, $\phi=90°$ and 75°, the dipolar contribution to

TABLE II. Results from MC–*NPT* simulations of dipolar rodlike molecules with $\phi=75°$, position $d^*=1$, and module $\mu^*=1$. See Table I for additional details. The biaxial order parameter $\langle R_{22}^2\rangle$ and the layer normal tilt angle $\langle \theta\rangle$ were zero at all temperatures studied.

T^*	$\langle U_{ij}^{GB}{}^*\rangle$	$\langle U_{ij}^{dd}{}^*\rangle$	$\langle R_{00}^2\rangle$	$\langle \psi_6\rangle$	Phase
2.1	-17.6 ± 0.2	-3.8 ± 0.1	0.97 ± 0.01	0.67 ± 0.02	S_B
2.2	-19.2 ± 0.2	-3.5 ± 0.1	0.97 ± 0.01	0.65 ± 0.02	S_B
2.3	-17.7 ± 0.2	-3.3 ± 0.1	0.96 ± 0.01	0.64 ± 0.02	S_B
2.4	-13.0 ± 0.1	-3.1 ± 0.1	0.96 ± 0.01	0.63 ± 0.02	S_B
2.5	-12.6 ± 0.1	-2.9 ± 0.1	0.95 ± 0.01	0.60 ± 0.02	S_B
2.6	-8.8 ± 0.1	-2.3 ± 0.1	0.85 ± 0.01		N
2.7	-7.7 ± 0.1	-2.0 ± 0.1	0.83 ± 0.01		N
2.8	-6.8 ± 0.1	-1.8 ± 0.1	0.79 ± 0.01		N
2.9	-6.3 ± 0.1	-1.7 ± 0.1	0.75 ± 0.01		N
3.0	-5.2 ± 0.1	-1.6 ± 0.1	0.68 ± 0.01		N
3.1	-3.2 ± 0.1	-1.5 ± 0.1	0.2 ± 0.01		I
3.2	-3.0 ± 0.1	-1.4 ± 0.1	0.1 ± 0.01		I
3.3	-2.8 ± 0.1	-1.3 ± 0.1	0.1 ± 0.01		I

TABLE III. Results from MC–*NPT* simulations of a system of dipolar rodlike molecules with $\phi=60°$, position $d^*=1$, and module $\mu^*=1$. See Table I for additional details.

T^*	$\langle U_{ij}^{GB*}\rangle$	$\langle U_{ij}^{dd*}\rangle$	$\langle R_{00}^2\rangle$	$\langle R_{22}^2\rangle$	$\langle\theta\rangle$	$\langle\psi_6\rangle$	Phase
1.7	-14.7 ± 0.2	-3.7 ± 0.1	0.98 ± 0.01	0.09 ± 0.02	4.7 ± 0.2	0.73 ± 0.02	S_J
1.8	-14.5 ± 0.2	-3.4 ± 0.1	0.97 ± 0.01	0.07 ± 0.02	4.8 ± 0.2	0.72 ± 0.02	S_J
1.9	-14.2 ± 0.2	-3.1 ± 0.1	0.97 ± 0.01	0.06 ± 0.02	4.6 ± 0.2	0.70 ± 0.02	S_J
2.0	-13.8 ± 0.2	-2.8 ± 0.1	0.97 ± 0.01	0.05 ± 0.02	4.6 ± 0.2	0.69 ± 0.02	S_J
2.1	-13.4 ± 0.2	-2.6 ± 0.1	0.97 ± 0.01	0.04 ± 0.02	3.8 ± 0.2	0.67 ± 0.02	S_J
2.2	-13.0 ± 0.2	-2.4 ± 0.1	0.96 ± 0.01	0.04 ± 0.02	3.6 ± 0.2	0.62 ± 0.02	S_J
2.3	-9.6 ± 0.2	-2.2 ± 0.1	0.91 ± 0.01				N
2.4	-8.9 ± 0.2	-1.9 ± 0.1	0.89 ± 0.01				N
2.5	-8.2 ± 0.2	-1.8 ± 0.1	0.87 ± 0.01				N
2.6	-7.7 ± 0.2	-1.7 ± 0.1	0.85 ± 0.01				N
2.7	-7.1 ± 0.2	-1.6 ± 0.1	0.81 ± 0.01				N
2.8	-6.6 ± 0.2	-1.5 ± 0.1	0.79 ± 0.01				N
2.9	-5.6 ± 0.2	-1.4 ± 0.1	0.65 ± 0.01				N
3.0	-3.1 ± 0.2	-1.3 ± 0.1	0.2 ± 0.01				I
3.2	-3.0 ± 0.2	-1.2 ± 0.1	0.1 ± 0.01				I

the energy varies smoothly across the isotropic-nematic and nematic-smectic transitions, while the GB curve shows, in correspondence of the phase changes, a significantly more marked variation. Thus, the molecular reorganization accompanying the transitions does not correspond to a relevant change of arrangement of the dipoles.

When the dipole point at 60° from the rod axis, tilted smectic phases are eventually observed [Figs. 9(a) and 10(a)]. For $d^*=1$, we have a nematic followed by a tilted smectic (see Fig. 5), while just moving the dipoles toward the terminal part of our ellipsoidal molecule, to the position $d^*=1.2$, the nematic phase is not observed anymore and we have a direct isotropic-tilted smectic transition, with a strong smectic stabilization (Fig. 6). This seems to be due to the easier possibility of interdigitation and to the related dipolar pairing allowed in this case. Indeed in this instance, the dipolar contribution to the energy is greatly increased by a factor of four [Fig. 6(a)] and correspondingly a large biaxiality [Fig. 6(b)] is also observed. Examining the radial distribution $g_0(r)$ of these $\phi=60°$ cases [Figs. 9(b) and 10(b)], we see that three peaks appear between $r^*=0$ and $r^*=3$ (excluded) at $d^*=1$, while an additional peak at $r^*=2.8$ appears for $d^*=1.2$. The assignment of the $g_0(r)$ peaks, reported in Figs. 9(c) and 10(c), indicates that the origin of the peaks corresponds to an interdigitated arrangement. We also see from Figs. 9(c) and 10(c) that the tilted phase has a local hexagonal structure, making it more similar to a tilted smectic-*B* phase than to a tilted smectic-*A* phase: the hexatic order for the $d^*=1$ case at $T^*=1.8$ is $\langle\psi_6\rangle\approx0.7$, while for the $d^*=1.2$ case at $T^*=2.7$ is $\langle\psi_6\rangle\approx0.8$ (see Tables III, IV). The hexagonal structure does not have only local character, as we can see from the hexatic correlation $g_6(r)$ [Figs. 9(d) and 10(d)], that does not decay to zero, indicating a phase with long-range hexatic order. An analysis of the

TABLE IV. Results from MC–*NPT* simulations of a system of dipolar rodlike molecules with $\phi=60°$, position $d^*=1.2$, and module $\mu^*=1$. See Table I for additional details.

T^*	$\langle U_{ij}^{GB*}\rangle$	$\langle U_{ij}^{dd*}\rangle$	$\langle R_{00}^2\rangle$	$\langle R_{22}^2\rangle$	$\langle\theta\rangle$	$\langle\psi_6\rangle$	Phase
2.4	-13.0 ± 0.2	-17.2 ± 0.1	0.98 ± 0.01	0.39 ± 0.02	7.6 ± 0.2	0.81 ± 0.02	S_J
2.5	-12.9 ± 0.2	-16.8 ± 0.1	0.98 ± 0.01	0.38 ± 0.02	7.6 ± 0.2	0.80 ± 0.02	S_J
2.6	-12.8 ± 0.2	-16.5 ± 0.1	0.98 ± 0.01	0.38 ± 0.02	7.7 ± 0.2	0.79 ± 0.02	S_J
2.7	-12.7 ± 0.2	-16.1 ± 0.1	0.97 ± 0.01	0.37 ± 0.02	7.7 ± 0.2	0.79 ± 0.02	S_J
2.8	-12.6 ± 0.2	-15.7 ± 0.1	0.97 ± 0.01	0.36 ± 0.02	7.5 ± 0.2	0.78 ± 0.02	S_J
2.9	-12.5 ± 0.2	-15.2 ± 0.1	0.96 ± 0.01	0.34 ± 0.02	7.3 ± 0.2	0.77 ± 0.02	S_J
2.95	-12.4 ± 0.2	-14.6 ± 0.1	0.94 ± 0.01	0.29 ± 0.02	7.1 ± 0.2	0.77 ± 0.02	S_J
2.98	-3.8 ± 0.2	-6.2 ± 0.1	0.20 ± 0.01				I
3.0	-1.9 ± 0.2	-6.1 ± 0.1	0.13 ± 0.01				I
3.2	-1.8 ± 0.2	-6.0 ± 0.1	0.1 ± 0.01				I
3.3	-1.7 ± 0.2	-5.6 ± 0.1	0.1 ± 0.01				I
3.4	-1.6 ± 0.2	-4.5 ± 0.1	0.1 ± 0.01				I
3.6	-1.6 ± 0.2	-4.0 ± 0.1	0.1 ± 0.01				I

TABLE V. Results from MC–*NPT* simulations of a system of dipolar rodlike molecules with $\phi=0°$, position $d^*=1$, and module $\mu^*=1$. See Table I for details. The $\langle R_{22}^2\rangle$ order parameter was zero at all temperatures studied.

T^*	$\langle U_{ij}^{GB}{}^*\rangle$	$\langle U_{ij}^{dd}{}^*\rangle$	$\langle R_{00}^2\rangle$	$\langle\theta\rangle$	$\langle\psi_4\rangle$	Phase
1.9	-14.4 ± 0.2	-4.3 ± 0.1	0.98 ± 0.01	8.1 ± 0.2	0.88 ± 0.02	S_T
2.0	-14.2 ± 0.2	-4.2 ± 0.1	0.98 ± 0.01	8.2 ± 0.2	0.87 ± 0.02	S_T
2.1	-14.0 ± 0.2	-4.1 ± 0.1	0.98 ± 0.01	8.1 ± 0.2	0.85 ± 0.02	S_T
2.2	-13.8 ± 0.2	-4.0 ± 0.1	0.97 ± 0.01	8.0 ± 0.2	0.84 ± 0.02	S_T
2.3	-8.7 ± 0.2	-1.1 ± 0.1	0.91 ± 0.01			N
2.4	-8.2 ± 0.2	-1.0 ± 0.1	0.89 ± 0.01			N
2.5	-8.0 ± 0.2	-1.0 ± 0.1	0.87 ± 0.01			N
2.6	-7.5 ± 0.2	-0.9 ± 0.1	0.85 ± 0.01			N
2.7	-7.1 ± 0.2	-0.9 ± 0.1	0.83 ± 0.01			N
2.8	-6.7 ± 0.2	-0.8 ± 0.1	0.80 ± 0.01			N
2.9	-6.2 ± 0.2	-0.8 ± 0.1	0.77 ± 0.01			N
3.0	-5.5 ± 0.2	-0.7 ± 0.1	0.69 ± 0.01			I
3.1	-3.1 ± 0.2	-0.6 ± 0.1	0.10 ± 0.01			I
3.2	-2.8 ± 0.2	-0.6 ± 0.1	0.10 ± 0.01			I
3.4	-2.6 ± 0.2	-0.5 ± 0.1	0.10 ± 0.01			I

samples shows that the tilt is in the direction of a vertex of the hexagon formed by the nearest neighbors. On the whole, we thus assign these phases as smectic-J phase [35].

The fluidity of the systems is monitored by the mean square displacements of centers of mass $\langle l_X\rangle$, $\langle l_Y\rangle$ and $\langle l_Z\rangle$ and the angular correlation function, associated with the spinning motion around the molecular long axis, $\langle C_x(n_c)\rangle = \langle \mathbf{x}(0)\cdot\mathbf{x}(n_c)\rangle$, where x is a transversal molecular axis and n_c is the number of elapsed cycles. Even if we do not have the true dynamics of the system available since we perform MC simulations, we can still consider these as useful indicators. Thus, if the Markov process updating the configuration is made of physical moves (e.g., if we perform runs where orientations are updated only by small angular steps and not also by 180° flips), we can use orientational correlation functions and mean square angular displacements to see if spinning takes place or if accepted moves are essentially frozen with respect to this type of motion. The $d^*=1$ system is fairly fluid in the nematic [Fig. 11(a)] but not much in the smectic, even if dipole reorientation around the long axis is still possible as we see from the angular correlation function $\langle C_x(n_c)\rangle$, shown in Fig. 11(b).

The final case treated of antiparallel axial dipoles ($\phi=0°$) shows yet another different picture. The dipolar contribution to the energy is fairly constant in the isotropic and nematic phases and jumps on going to the tilted smectic [Fig. 7(a)], even if the total contribution is much smaller than in the previous case and comparable to that of the $\phi=60°$, $d^*=1$ case. As we can see from the snapshot in Fig. 12(a) and from the radial distribution, Fig. 12(b), the structure of

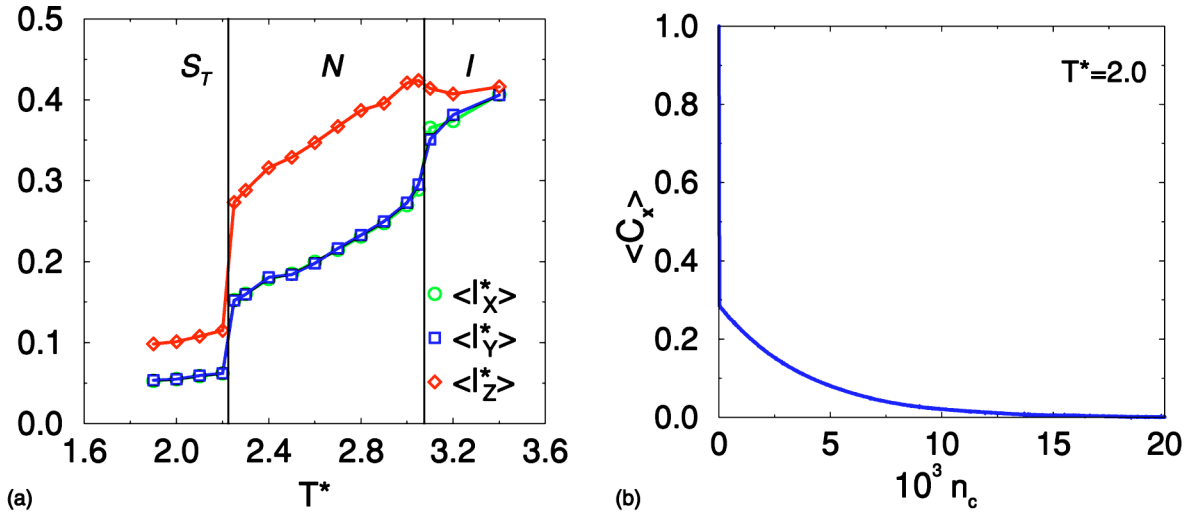

FIG. 13. Averages mean square displacements $\langle l_X^*\rangle$, $\langle l_Y^*\rangle$, and $\langle l_Z^*\rangle$ (a) and autocorrelation function for reorientation around the molecular axis $\langle C_x\rangle$ at $T^*=2.0$ (b), for the case $\phi=0°$ and $d^*=1.0$.

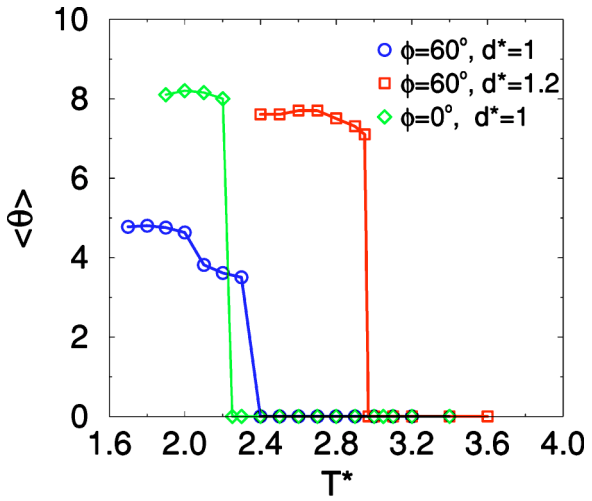

FIG. 14. Average tilt angle $\langle\theta\rangle$ (measured in degrees) of the layers with respect to the director as a function of temperature for the cases $\phi=60°$, $d^*=1.0$ and $\phi=60°$, $d^*=1.2$, and $\phi=0°$, $d^*=1.0$.

the tilted phase is now strikingly changed. Neighboring layers are strongly interdigitated and the peak at $r^*=3$ of $g_0(r)$ is now disappeared showing the little relevance of end-to-end configurations compared to the not interdigitated ones shown in Figs. 9(a) and 10(a). Moreover, the local layer structure is now tetragonal, with four rather than six neighbors in the first and second shells [Fig. 12(c)], that we have indicated with smectic-*T* phase (S_T). We can introduce a tetragonal bond order parameter ψ_4 analogous to the ψ_6 defined in Eqs. (4) and (5) and again by analogy with Eq. (6) a spatial correlation $g_4(r)$. We find the quite high values of $\langle\psi_4\rangle$ reported in Table V and the correlation $g_4(r)$ in Fig. 12(d). Figure 13(a) shows a mean square displacement similar to that of Fig. 11(a), and Fig. 13(b) evidences an autocorrelation function $\langle C_x(n_c)\rangle$ which decays noticeably faster than the $\phi=60°$ case [cf. Fig. 11(b)].

It is worth mentioning the case of tilted smectics obtained from axial quadrupolar GB particles by Neal and co-workers [37], particularly since our two separated dipoles do give a quadrupole contribution when a multipole expansion of their charge distribution is performed. We notice, however, that our GB dipolar potential is significantly different and can correspond to the point quadrupole only if we let the separation of the dipoles tend to zero. Two separated, off-center dipoles offer possibilities of interdigitation, with pairing of opposite dipoles across layers, that we have already shown to be important here and even in determining phase organization in the case of single dipoles [18]. Indeed, as the separation gets larger, the phase behavior changes. Figs. 5 and 6 exhibit this: for $d^*=1$, the system shows isotropic, nematic, and smectic-*J* phases, while an incrementation of the separation to $d^*=1.2$ suppresses the nematic phase and the system goes directly from isotropic into the smectic-*J* phase.

Finally, Fig. 14 shows the average $\langle\theta\rangle$ tilt angles, we have observed, as a function of temperature. In all systems, we have studied the tilted phase was an alternative to the upright smectic-*B* phase, as in no case both were observed. For all models, the tilt angle observed was smaller than 10° and with little dependence on temperature.

We notice that in no case a truly smectic-*C* phase, with no structure inside the layers, is observed. This might be due to our choice of parameters or to a limitation of the rigid GB model with two dipoles. In fact, if on one hand the long-range nature of dipolar interactions might provide the structuring, on the other, in most *C* smectogens the structure consists of a core with a chain at each end which might help in reducing the coherence of mesogens in the plane by effectively ''insulating'' them. It should be interesting to test this hypothesis by adding terminal chains although this would considerably increase the complexity of the model.

V. CONCLUSIONS

We have simulated systems of molecules with two outboard permanent dipoles at various angles from the axis. We have observed tilted smectic phases for a Gay-Berne system with two tilted outward-pointing dipoles when the dipole orientation is sufficiently close to the long molecular axis. The smectic phases show in all cases some layer structuring that is hexagonal when dipoles are at 60°, indicating a smectic-*J* phase, and tetragonal smectic-*T* phase for axial dipoles.

ACKNOWLEDGMENTS

We are grateful to EU TMR (Contract No. FMRX–CT97–0121), University of Bologna, CNR, and INSTM for financial support towards the computer resources employed.

[1] G.W. Gray and J.W. Goodby, Smectic Liquid Crystals, *Textures and structures* (Leonard Hill, Glasgow, 1984).
[2] G. Vertogen and W.H. de Jeu, *Thermotropic Liquid Crystals* (Springer-Verlag, Berlin, 1988).
[3] P.J. Collings and M. Hird, *Introduction to Liquid Crystals* (Taylor and Francis, London, 1997).
[4] W.L. McMillan, Phys. Rev. A **8**, 1921 (1973).
[5] A. Michelson, D. Cabib, and L. Benguigui, J. Phys. (Paris) **38**, 961 (1977).
[6] B.W. van der Meer and G. Vertogen, J. Phys. Colloq. **40**, C3-222 (1979).
[7] M. Matsushita, J. Phys. Soc. Jpn. **50**, 1351 (1981).
[8] W.J.A. Goossens, Phys. Rev. A **40**, 4019 (1989).
[9] A.S. Govind and N.V. Madhusudana, Europhys. Lett. **55**, 505 (2001).
[10] J.W. Goodby, G.W. Gray, and D.G. McDonnel, Mol. Cryst. Liq. Cryst. **34**, 183 (1977).
[11] Z. Luz and S. Meiboom, J. Chem. Phys. **59**, 275 (1973).
[12] H. Hervet, F. Volino, A.J. Dianoux, and R.E. Lechner, Phys. Rev. Lett. **34**, 451 (1975).
[13] M.A. Glaser, R. Malzbender, N.A. Clark, and D. Walba, J. Phys.: Condens. Matter **6**, A261 (1994).

[14] W.G. Jang, M.A. Glaser, C.S. Park, K.H. Kim, Y. Lansac, and N.A. Clark, Phys. Rev. E **64**, 51712 (2001).
[15] J.G. Gay and B.J. Berne, J. Chem. Phys. **74**, 3316 (1981).
[16] D.J. Adams, G.R. Luckhurst, and R.W. Phippen, Mol. Phys. **61**, 1575 (1987).
[17] C. Zannoni, J. Mater. Chem. **11**, 2637 (2001).
[18] R. Berardi, S. Orlandi, and C. Zannoni, Chem. Phys. Lett. **261**, 357 (1996).
[19] R. Berardi, S. Orlandi, D.J. Photinos, A. Vanakaras, and C. Zannoni, Phys. Chem. Chem. Phys. **4**, 770 (2002).
[20] K. Satoh, S. Mita, and S. Kondo, Chem. Phys. Lett. **255**, 99 (1996).
[21] E. Gwozdz, A. Brodka, and F. Pasterny, Chem. Phys. Lett. **267**, 557 (1997).
[22] E. Gwozdz, A. Brodka, and F. Pasterny, J. Mol. Struct. **555**, 257 (2000).
[23] A. Gil-Vilegas, S.C. McGrother, and G. Jackson, Mol. Phys. **92**, 723 (1997).
[24] M. Houssa, A. Oualid, and L.F. Rull, Mol. Phys. **94**, 439 (1998).
[25] R. Berardi, S. Orlandi, and C. Zannoni, Int. J. Mod. Phys. C **10**, 477 (1999).
[26] R. Berardi, S. Orlandi, and C. Zannoni, Phys. Chem. Chem. Phys. **2**, 2933 (2000).
[27] E. de Miguel, L.F. Rull, M.K. Chalam, and K.E. Gubbins, Mol. Phys. **74**, 405 (1991).
[28] M.A. Bates and G.R. Luckhurst, Struct. Bonding (Berlin) **94**, 66 (1999).
[29] A. Wulf, Phys. Rev. A **11**, 36 (1975).
[30] R. Bartolino, J. Doucet, and G. Durand, Ann. Phys. (Leipzig) **3**, 389 (1978).
[31] D.J. Photinos and E.T. Samulski, Science **270**, 783 (1995).
[32] M.P. Neal, A.J. Parker, and C.M. Care, Mol. Phys. **91**, 603 (1997).
[33] A.G. Vanakaras, D.J. Photinos, and E.T. Samulski, Phys. Rev. E **57**, 4875 (1998).
[34] J. Xu, R.L.B. Selinger, J.V. Selinger, B.R. Ratna, and R. Shashidhar, Phys. Rev. E **60**, 5584 (1999).
[35] I.M. Withers, C.M. Care, M.P. Neal, and D.J. Cleaver, Mol. Phys. **100**, 1911 (2002).
[36] M.P. Neal and A.J. Parker, Phys. Rev. E **63**, 11706 (2000).
[37] M.P. Neal and A.J. Parker, Chem. Phys. Lett. **294**, 277 (1998).
[38] A. Poniewierski and T.J. Sluckin, Mol. Phys. **73**, 199 (1991).
[39] G. Barbero and G. Durand, Mol. Cryst. Liq. Cryst. **179**, 199 (1990).
[40] R. Berardi, A.P.J. Emerson, and C. Zannoni, J. Chem. Soc., Faraday Trans. **89**, 4096 (1993).
[41] J.A. Barker and R.O. Watts, Mol. Phys. **26**, 789 (1973).
[42] F. Biscarini, C. Chiccoli, P. Pasini, F. Semeria, and C. Zannoni, Phys. Rev. Lett. **75**, 1803 (1995).
[43] R. Berardi and C. Zannoni, J. Chem. Phys. **113**, 5971 (2000).
[44] A. Jaster, Phys. Rev. E **59**, 2594 (1999).